Physica D 238 (2009) 1152–1160

Contents lists available at ScienceDirect

Physica D

journal homepage: www.elsevier.com/locate/physd

A low-dimensional model of separation bubbles

R. Krechetnikov [a,*], J.E. Marsden [b], H.M. Nagib [c]

[a] Department of Mechanical Engineering, University of California at Santa Barbara, Santa Barbara, United States
[b] Control & Dynamical Systems, California Institute of Technology, Pasadena, United States
[c] Mechanical, Materials, and Aerospace Engineering Department, Illinois Institute of Technology, Chicago, United States

ARTICLE INFO

Article history:
Received 8 October 2007
Received in revised form
23 May 2008
Accepted 22 March 2009
Available online 8 April 2009
Communicated by M. Silber

Keywords:
Separation bubble
Flow separation control
Low-dimensional modeling
Singularity theory
Phenomenology

ABSTRACT

In this work, motivated by the problem of model-based predictive control of separated flows, we identify the key variables and the requirements on a model-based observer and construct a prototype low-dimensional model to be embedded in control applications.

Namely, using a phenomenological physics-based approach and dynamical systems and singularity theories, we uncover the low-dimensional nature of the complex dynamics of actuated separated flows and capture the crucial bifurcation and hysteresis inherent in separation phenomena. This new look at the problem naturally leads to several important implications, such as, firstly, uncovering the physical mechanisms for hysteresis, secondly, predicting a finite amplitude instability of the bubble, and, thirdly, to new issues to be studied theoretically and tested experimentally.

1. Introduction

1.1. Motivation and objective

In recent years there has been an increasing demand to extend the range of aircrafts' flight conditions to high angle-of-attack regimes and high-amplitude maneuvers. The latter usually lead to intense flow separation and dynamic vortex shedding which in turn generate destructive pitching moments, sharp increases in drag, and losses in lift. Therefore, the only way to enlarge the flight envelope is to design efficient ways of controlling flow separation. The classical approach is based on open-loop control, which is achieved either by mechanical or fluidic actuation according to operating schedules (lookup tables) constructed using extensive and costly experimental studies. On the other hand, feedback control schemes do not require operating schedules and, being more efficient and reliable [1], also naturally allow one to address the optimization issue.

However, feedback control is more demanding theoretically since it requires an embedded model which predicts the behavior of the physical system at hand. In the case of flow separation, the general equations of fluid motion – the Navier–Stokes equations (NSEs) – are known and can, in principle, produce accurate prediction of the flow structure, but because the real boundary and initial conditions are noisy and cannot be precisely measured and because the NSEs cannot be solved in real time in flight, this approach is impractical. However, an accurate real-time solution is not actually necessary, since in reality one can use sensors on the boundary of lifting surfaces, which in turn read off a certain amount of extra information from the physical system and therefore should allow one to weaken the requirements on the model accuracy. Thus, one is naturally led to look for *coarse* models, which should also be *low dimensional* for computational real-time efficiency. Construction of such models is the main objective of our work.

Historically, the importance of low-dimensional modeling of unsteady aerodynamic characteristics – aerodynamic forces and moments acting on an aircraft – for control purposes, stability analysis, and dynamic simulations has been realized for a long time and the appropriate models were developed; see, for example, [2–7]. However, the necessity to model the separation and vortex shedding dynamics was realized just recently in view of the increasing demand for high angle-of-attack regimes [2]. Early attempts to develop dynamical models are based on the anzatz that the phenomenon of flow separation behaves linearly for small variations of the parameters involved [5–7], which has many limitations, as will be clear from the subsequent discussion when we establish the requirements on a model aimed for robust control.

* Corresponding author.
E-mail address: rkrechet@cds.caltech.edu (R. Krechetnikov).

0167-2789/$ – see front matter © 2009 Elsevier B.V. All rights reserved.
doi:10.1016/j.physd.2009.03.017

1.2. Previous works

In one of the early works, [2], the coordinate of a separation point $x \in [0, 1]$ is taken as an internal state-space variable and the ad hoc linear first-order equation is used to account for the movement of the separation point for unsteady flow conditions:

$$\tau_1 \frac{dx}{dt} + x = x_0(\alpha - \tau_2 \dot{\alpha}),$$

where we kept the original notations: τ_i are relaxation times, and $x_0(\alpha)$ is the stationary value of the separation point position for a given angle of attack α. Then the value $x = 1$ corresponds to attached flow, while $x = 0$ corresponds to leading edge separation. A similar approach was used in the construction of the models for separation phenomena, for example, [5] and the ONERA model [6]. In particular, the key feature of the state-of-the-art low-dimensional model used in a closed-loop control of dynamic stall with pulsed vortex generator jets due to Magill et al. [5] is a choice of the governing physical parameters, such as lift Z and separation state B with $B = 0$ corresponding to fully attached flow and $B = 1$ to fully separated flow. Steady states, $B_s(\alpha)$ and $Z_s(\alpha)$, represent the baseline case and the measured steady lift, respectively, as functions of the angle of attack α. The experimentally measured function $Z_s(\alpha)$ may contain a hysteretic behavior and thus is an empirical way of accounting for a hysteresis, as suggested by Magill et al. [5]. Exploiting the physical arguments: (i) lift $Z \sim$ circulation $\Gamma(\alpha)$; (ii) relaxation to a baseline state $\lim_{t\to+\infty} B(t) = B_s(\alpha)$; (iii) rise in lift when a dynamic vortex is shed $Z \sim B_t$, one arrives at the simplest low-order model with adjustable parameters,

$$B_{tt} = -k_1 B_t + k_2 [B_s(\alpha) - B], \tag{1a}$$

$$Z_t = k_3 B_{tt} + k_4 [Z_s(\alpha) - Z] + \Gamma_\alpha \alpha_t. \tag{1b}$$

As one can notice, all these models are linear.

In the case of aerodynamic models for forces and moments, the addition of nonlinear terms is known to extend the range of flight conditions to high angle-of-attack regimes and maneuvers [4], which is usually done in an ad hoc manner, by simply adding polynomial terms with unknown coefficients without any physical insight or justification. Systematic application of local and global bifurcation theories to the aerodynamic models is just beginning to be appreciated [3]. To the authors' knowledge there have been no similar attempts in these directions for models of flow separation. In fact, the systematic methods available to formulate such models are very limited and the connection of known models to physics is rather far from desired. A commonly used approach is to first generate experimental data and then to extract the model by a projection onto proper orthogonal decomposition (POD) modes using, for example, balanced truncation or similar methods. This technique is known to be incapable of capturing the dynamics with a few modes for the wide range of governing parameters in view of the open flow nature of the problem, in particular. In addition, while POD models are based on the most energetic modes, they do not provide deep insights into the physics of the flow.

1.3. Model requirements and methodology

In this work we develop a model which is not a mnemonic device encoding the experimental observations, as ad hoc models would be, but is *physically motivated* and thus is more robust in reflecting the actual behavior for a wide range of flight and control parameters.

In view of the necessary coarse nature of the model and the application objectives, one has to decide which aspects of the dynamics should be modeled reasonably accurately. With the target of producing a model, upon which an observer in a closed-loop control scheme can be based for a wide range of physical parameters, in this work we identify the crucial elements of the dynamics of separation bubble, namely *bifurcation* and *hysteresis*, which need to be reflected in the model. These elements reflect the fundamental *nonlinear* nature of the physical problem, which apparently cannot be captured with linear models.

As follows from the above discussion, being nonlinear, low dimensional, and physically motivated are *key requirements* for a model. In this work, we shall make use of *phenomenological* modeling, which has been successful in many other problems, such as Duffing's equation for the buckling of elastic beams [8], simple maps to describe a dripping faucet [9], which even capture the observed chaotic behavior to a great extent, and bubble dynamics in time periodic straining flows [10], to name a few. As will be clear from the text later, besides appealing to a phenomenological physically motivated analysis of empirical facts we also provide a basis for it in dynamical systems and singularity theories. A symbiosis of these two methodologies yields a coherent picture of the phenomena. It should also be stressed that in view of the coarse nature of the model that is sought, we effectively construct an "approximate global normal form", which reflects the key global features of the physical system, necessary for control purposes.

1.4. Paper outline

To achieve the above objectives, we first will identify the central idea of our approach in Section 2, and then appeal to the tools of the bifurcation and singularity theory [11], as will be made precise in Section 3. The outline of the paper is as follows. In Section 3, we discuss the first nonlinear aspect of separation bubbles, namely the bifurcation phenomenon and the way to model it. In Section 4, we explore the basic physics of hysteresis phenomena, and suggest a single model capable of capturing both bifurcation and hysteresis.

2. Central idea

A central notion and object, whose dynamics we study, is *a separation bubble*, whose main features are as follows. First of all, separation of the boundary layer develops due to an adverse pressure gradient [12] which occurs when the angle of attack of an airfoil is sufficiently large, see Fig. 1(a), and may be followed by re-attachment as in Fig. 1(b), thus forming a typical flow around an airfoil. The region encompassed by the boundary layer is termed a separation bubble after the work of Jones [13] and, as shown in Fig. 1, it can be closed or open. Classification of separation bubbles concerns their laminar or turbulent nature, but at a coarse level topologically laminar and turbulent bubbles do not differ, and thus we will not be distinguishing between various cases, but rather treat a generic case. It should be noted that, in certain physical situations, a bubble needs to be understood in a time-averaged sense [14]. Given the notion of a separation bubble, our dynamical systems model will aim to capture its characteristics, which are important for controlling separation phenomena.

A central idea of this work is to approach the modeling of separation bubble phenomena by identifying the key crucial elements of the bubble dynamics, namely bifurcations and hysteresis, in the appropriate portion of configuration space, as sketched in Fig. 2. In this figure we show the minimal dimension of the *configuration space*, defined by the bubble size x, the angle of attack α, and the actuation amplitude w; that is, we will be looking for the minimal model determined by the dependence of the bubble size on the angle of attack and actuation amplitude.

This minimal dimension is motivated by the fact that while generally there are other parameters involved, such as the Reynolds number Re, the critical angle of attack α_c, and the airfoil thickness h, the resulting model will still have wide applicability. This can be understood based on the aerodynamic properties

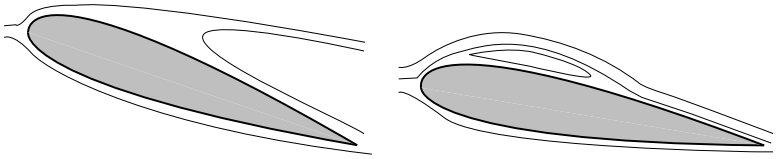

(a) Separated flow: Open bubble. (b) Re-attached flow: Closed bubble.

Fig. 1. On the notion of separation bubble.

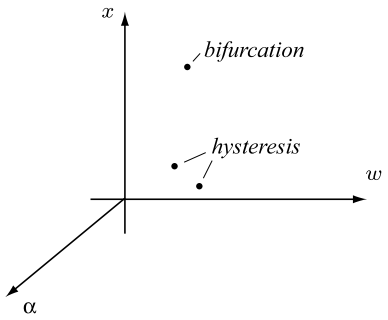

Fig. 2. A sketch of the key dynamic elements—bifurcation and hysteresis—to be captured by the minimal number of parameters, namely the bubble size x, the angle of attack α, and the actuation amplitude w.

of airfoils. To explain this, we draw critical curves, i.e., when separation takes place depending upon Re, α_c, and h in Fig. 3.

As illustrated by Fig. 3(a), in the case of real airfoils, separation occurs at finite Reynolds numbers even at zero critical angle of attack; the higher α_c the lower the critical Reynolds number Re_c; also, the thicker the airfoil, the lower Re_c. Fig. 3(b) demonstrates the fact that the thinner an airfoil, the larger the critical angle of attack that is required to achieve separation at a given Reynolds number Re^*. Finally, in the α_c–Re plane in Fig. 3(c) one can observe that, for fixed airfoil thickness h^*, separation can occur at zero α_c, which requires high enough Reynolds numbers. Since in reality the Reynolds numbers are huge (e.g. for real aircraft Re varies between 10^6 and 10^{11}), one concludes that limiting ourselves to "thick airfoils", which can, in fact, be regarded as real airfoils since they have to carry structural load and fuel, is not a serious restriction in this first step towards low-dimensional modeling of separation phenomena.

Having identified the key elements of the bubble dynamics in the configuration space, we construct a model by successively addressing bifurcation phenomena in Section 3 and hysteresis phenomena in Section 4.

3. Bifurcation in the dynamics of separation bubble

3.1. On the notion of bifurcation

As was noted in Section 2, bubbles can be either in a closed or open state. This allows us to introduce the first key element of the low-dimensional modeling, namely it must capture this *basic bifurcation* from an *open* to a *closed* state, as shown schematically in Fig. 4, which is also known as *bursting* [15].

Notably, the fact that this is the primary bifurcation was realized just recently [16]. While from the vast literature one can get the impression that one separated flow is not like any other, here we take a different point of view, i.e. we treat the coarse behavior of separation bubbles as (generic) phenomena that can be modeled by a single low-dimensional dynamical system.

3.2. Quantifying separation bubbles

To quantify the behavior of a separation bubble, consider the coordinate x, measuring the distance along the airfoil from the bubble onset to the bubble reattachment, as shown in Fig. 4. The bubble dynamics in the first approximation can be described by two parameters: the location of separation, x_s, and of reattachment, x_r, which can move under the change of flight and control parameters. In some cases, e.g. the Glauert Glas II airfoils, the separation point x_s remains fixed for all practical purposes. Therefore, we will start by considering only the behavior of the reattachment point, which experiences a primary bifurcation in the above sense; extending the model to include variation of x_s will require the addition of a reliable separation criterion. As an alternative to x_r, one could also utilize the bubble area. From now on we will use x as a variable representing the bubble state.

3.3. On the physical nature of bifurcation

The mechanism by which the excitation affects the flow lies in the generation of instabilities, and thus of large coherent structures [17] transferring high momentum fluid towards the

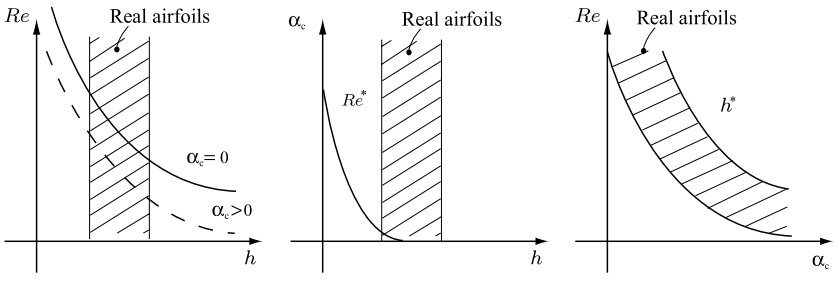

(a) Re vs. h for $\alpha_c = 0$ (solid curve) and $\alpha_c > 0$ (dashed curve). (b) α_c vs. h at fixed $Re = Re^*$. (c) Re vs. α_c at fixed $h = h^*$.

Fig. 3. The placement of real airfoils in the space defined by the Reynolds number Re, the critical angle of attack α_c, and the airfoil thickness h: the critical curves corresponding to the instant when separation occurs. Re^* and h^* are typical fixed values of these parameters.

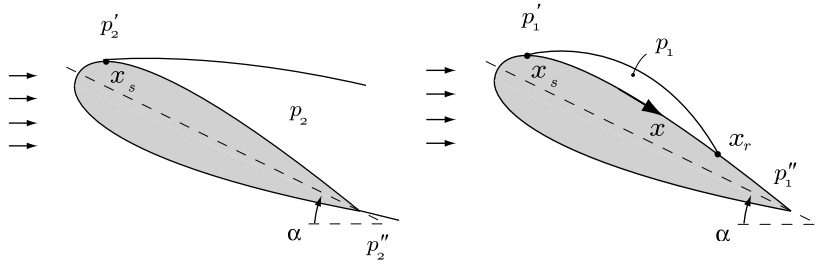

(a) Open bubble, $x_r = \infty$: Under-actuated case, $w < w_c$.

(b) Closed bubble, $x_r < \infty$: Controlled case, $w > w_c(\alpha)$.

Fig. 4. Basic setup and primary bifurcation.

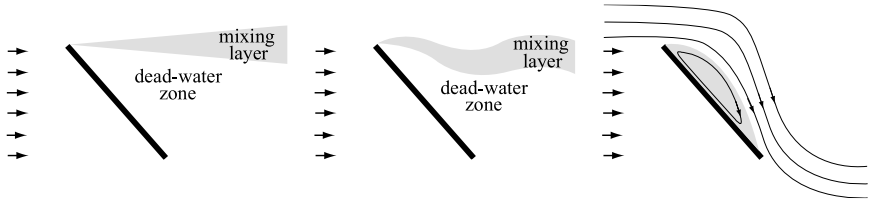

(a) No excitation. (b) Weak excitation. (c) Strong excitation.

Fig. 5. On the mechanism of actuation.

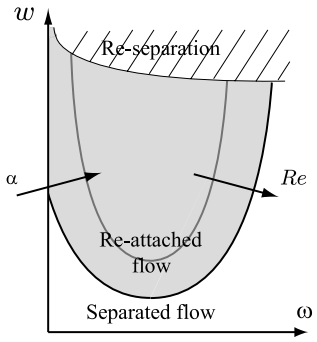

Fig. 6. Effect of time-varying actuation: criticality of the actuation amplitude w and the frequency ω. The shaded region corresponds to a reattached flow (closed bubble). Arrows indicate the change in location of the transition curve with increasing Re and α.

surface, see Fig. 5(b), and therefore leading to reattachment, as indicated in Fig. 5(c). Since actuation exploits the instabilities of the shear layer [18], the response to actuation depends on both amplitude w and frequency ω, and therefore is nonlinear. The latter again indicates, now from the point of view of actuation control mechanisms, that the low-dimensional model must be nonlinear. As follows from experiments with synthetic (zero mass flux) jet actuation, the critical phenomena are as sketched in Fig. 6, where the shaded region corresponds to a reattached flow (that is, a closed bubble) and the arrows indicate a change in location of the transition curve with an increase in α and Re, respectively. The size of the bubble, x, has a specific dependence on the amplitude w and frequency ω of actuation, *i.e.* $\partial x/\partial w < 0$, $\partial x/\partial \omega < 0$, when moving away from the origin $(w, \omega) = \mathbf{0}$ in Fig. 6. In this work we focus on the case of time-invariant actuation, $\omega = 0$, although the time-varying case will be commented on later in this section.

Finally, it is notable that the criticality and hysteresis phenomena depend on the connectedness of the flow domain: the bubble experiences bifurcation only in the case of flow around an airfoil, as in Fig. 7(b), while in the case of a hump model in Fig. 7(a), which is frequently used in experiments, e.g. [19], there is no bifurcation. Thus, there are two basic configurations in which the behavior of the separation bubble differs: the *hump model* and the *airfoil model*. Namely, in the hump case $x(w)$ is smooth, while in the case of an airfoil $x(w)$ is discontinuous. Also, as will be important in Section 3, the hysteresis phenomena are present only in the airfoil case. Here, in view of its practical importance, we naturally focus on the airfoil case.

3.4. Modeling the bubble bifurcation

In developing a model, we are guided by the principle of a minimal complexity together with the physical requirements one has to meet. At the methodological level, there are two basic ways to account for the form of $x(w)$, which has both the saturation and criticality shown in Fig. 7: (a) to design an *algebraic* relation $f(x, w) = 0$, or (b) to introduce a *dynamic* description $f(x, \dot{x}, \ddot{x}, \ldots, w) = 0$. The latter approach is better suited for dynamics and control purposes, because in the case of active feedback control one would need to deal with a few characteristic times and transient effects, and thus the model should be time dependent. The simplest possible way of introducing time-dependent dynamics is a second-order oscillator model,

$$\ddot{x} - \mu\dot{x} = F(x, w), \tag{2}$$

where μ is a damping parameter. The justification for the latter is the fact that both separation and reattachment points may oscillate [14].

In what follows, we first formulate the mathematical requirements on a model in Section 3.4.1, then, by appealing to the ideas of a potential function in Section 3.4.2 and a dynamic bifurcation in Section 3.4.3, we identify a specific form of model (2) in Section 3.4.4.

3.4.1. Mathematical requirements

Naturally, the bubble size x also depends on a *flight parameter*, in our case the angle of attack α, which needs to be incorporated in the model (2); thus, F in (2) in enhanced to $F(x, w, \alpha)$. Since we want to minimize the functional complexity but retain the true nonlinear features of the phenomena, the simplest form is a quadratic nonlinearity,

$$F(x, w, \alpha) = x^2 + b(w, \alpha)\, x + c(w, \alpha), \tag{3}$$

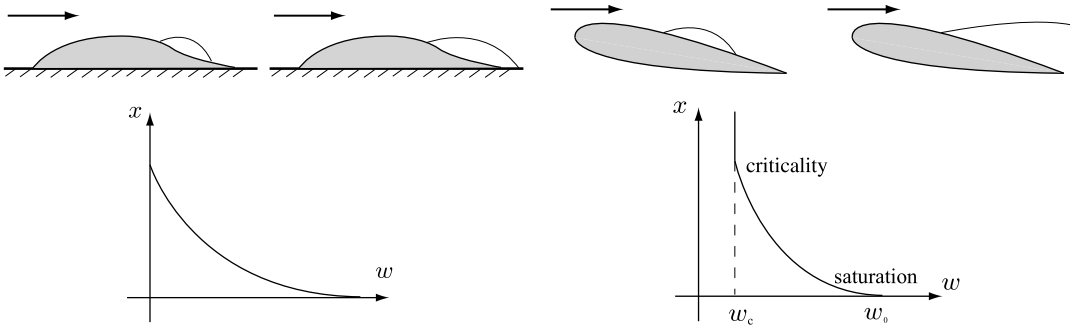

(a) Hump model: "half of an airfoil" mounted on a wall. (b) Airfoil model.

Fig. 7. Two basic experimental configurations.

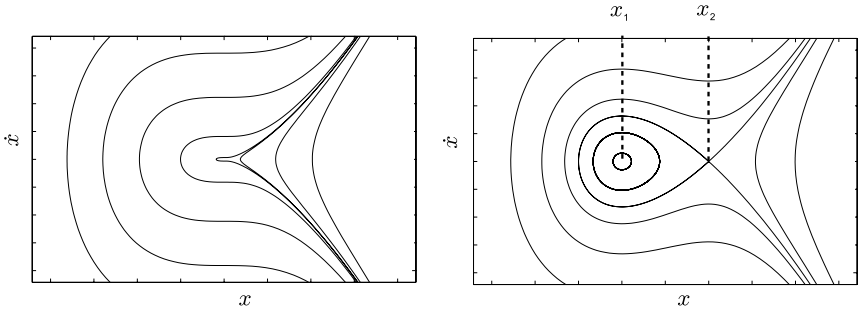

(a) Uncontrolled. (b) Controlled.

Fig. 8. Takens–Bogdanov bifurcation.

which will be justified by its physical implications and the potential function approach in Section 3.4.2. Eq. (2) with the nonlinearity given by (3) possesses a Takens–Bogdanov bifurcation, as shown in Fig. 8, when $b^2 - 4c$ changes sign.

Indeed, the equilibrium points are given by $x_{1,2} = -\frac{b}{2} \mp \frac{1}{2}\sqrt{b^2 - 4c}$, so that F can be represented as $(x - x_1)(x - x_2)$. The eigenvalues of the linearization around $x = x_1$ are defined by $\lambda^2_{(1)} = x_1 - x_2 = -\sqrt{b^2 - 4c}$, while the eigenvalues of the linearization around $x = x_2$ are $\lambda^2_{(2)} = x_2 - x_1 = \sqrt{b^2 - 4c}$. Thus when $b^2 - 4c$ changes sign, one observes the transition from the picture in Fig. 8(a) to the one in Fig. 8(b). The requirements on the parameters in this model are dictated by the physics:

(a) The stability of equilibria points should obey

$$\alpha < \alpha_c : b^2 - 4c > 0 \quad \text{(stability)},$$
$$\alpha > \alpha_c : w > w_c(\alpha),\ b^2 - 4c > 0$$
$$\text{(stability: no separation)},$$
$$w < w_c(\alpha),\ b^2 - 4c < 0 \quad \text{(instability: separation)},$$

where stability implies that one equilibrium is stable (λ is imaginary), and the second one is unstable (λ is real). The above inequalities indicate that the physical behavior of the model is also governed by the critical angle of attack α_c (which is defined when the flow separates at $w = 0$), and the critical control amplitude $w_c(\alpha)$, when flow reattaches at α fixed.

(b) The critical actuation amplitude w_c should grow with $(\alpha - \alpha_c)$, since the higher the angle of attack, the more control input is required to make the flow reattach.

(c) The bubble size x, which is a stable equilibrium, should shrink, $x \to 0$, as w increases. At the same time, the domain of attraction of this equilibrium should shrink too, so that the bubble becomes susceptible to a finite-amplitude instability, as is known to be the case from experiments; see the upper part of Fig. 6.

3.4.2. Potential function approach

In order to get better insight in the model construction, let us assign a potential function $V(x)$, where dependence on w and α is suppressed for the sake of this discussion, such that $V'(x) = -F(x)$:

$$V(x) = -\frac{x^3}{3} - b(w)\frac{x^2}{2} - c(w)x - d(w), \tag{4}$$

which is physically determined by the effective elastic properties of a bubble coming from its interaction with the outer flow. The elasticity of the separation bubble is evidenced by introducing disturbances outside the bubble and observing the changes in the bubble characteristics, i.e. shape and pressure inside.[1] Since the effective tension of the shear layer tends to maximize the bubble boundary by making it open and only the external energy input (excitation) counterparts this effect and makes the bubble closed, the separation bubble boundary elastic properties should be modeled with negative interfacial tension $-\widetilde{\sigma}$.[2] The latter is opposite to the behavior of real bubbles with positive interfacial tension, which usually tends to minimize the interfacial area.

Given this justification for the origin of the potential energy, we can next observe that a finite bubble corresponds to $V(x)$ as in Fig. 9(a), and an infinite bubble corresponds to Fig. 9(b). Therefore, now from an energetic point of view, we can conclude that a

[1] Both elasticity and a non-trivial state equation of the separation bubble have been confirmed experimentally (personal communication: John Kiedaisch, IIT).

[2] Alternatively, one can use a non-trivial state equation for the pressure inside the bubble, which can in principle be measured experimentally.

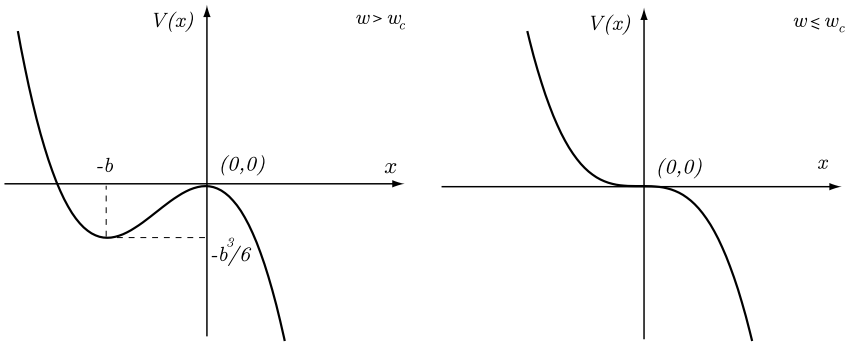

(a) Potential function for a finite bubble. (b) Potential function for an infinite bubble.

Fig. 9. Potential function $V(x)$; $d = 0$, $c = 0$ in (4).

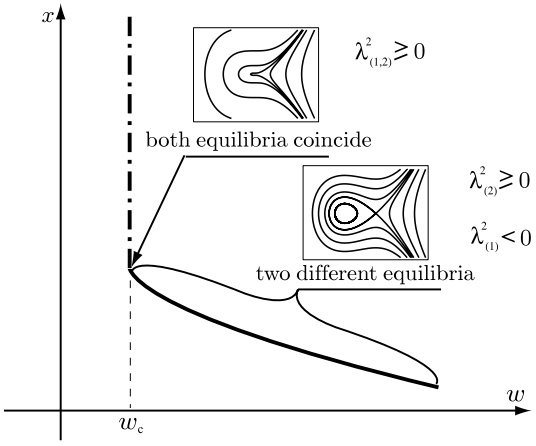

Fig. 10. Critical curve in the (x, w)-plane: on the dynamic bifurcation; the solid black line represents stable equilibria, the dot–dash line is a dynamic bifurcation when the bubble grows indefinitely with time. Phase portraits in rectangles correspond to the ones in Fig. 8.

quadratic nonlinearity (or cubic potential V) is adequate for the description of the bifurcation phenomenon (see also the discussion in Section 3.4.3).

Without loss of generality, we can assume that $d = 0$. Considering w as a control parameter, the requirements on the coefficients in $V(x)$ are such that the equilibria, $V'(x) = -x^2 - bx - c = 0$, obey

$$w > w_c : \text{ two equilibria (stable and unstable)}, \quad V''(x_1) > 0, \quad V''(x_2) < 0;$$

$$w \le w_c : \text{ only one equilibrium point, which is unstable (marginally stable)}.$$

The stability conditions can also be reformulated in terms of eigenvalues, as indicated in Fig. 10. For illustrative purposes, in the particular case when $c = 0$ the equilibria points $x_i(w, w_c)$ are easily computable: $x_1 = -b$ and $x_2 = 0$. The stability criterion (second variation) for these equilibria is given by the sign of the second derivative, $V''(x) = -2x - b$, which at the equilibria points assumes the values b and $-b$, respectively. Besides the stability conditions, one needs to impose $\mathrm{d}x_1/\mathrm{d}w < 0$, since the bubble shrinks when the control amplitude increases. Thus, the bifurcation from the state in Fig. 9(a) to the one in Fig. 9(b) is obviously associated with the condition when $b(w_c) = 0$.

In general, as one can further infer, in the space of curves in (w, w_c) there is an infinite number of solutions $b = b(w, w_c)$, $c = c(w, w_c)$. In practice, a systematic procedure would be as follows: depending on the particularities of the experimental data, one expands b and c in terms of some basis functions of w, w_c, etc., and then determines coefficients in that expansion through a calibration procedure based on experimental data. The latter procedure is, in fact, used in aerodynamic models (i.e. connecting forces and moments) [4,20].

3.4.3. Dynamic bifurcation

The transition from one potential to another is controlled by a bifurcation parameter, such as angle of attack α or actuation amplitude w. In fact, the latter two parameters are interchangeable to a certain extent as argued in [21], since a change in α or in w leads to a change in circulation around an airfoil, and thus to a change in the flow structure. Apparently, this transition of x from finite to infinite is *dynamic* in the sense that the bubble becomes infinite in Fig. 9(b) as time $t \to \infty$. This dynamic bifurcation can be clarified using phase portraits in Fig. 10, and should be compared to the standard static bifurcation, which is of algebraic nature, resulting from the condition of vanishing vector fields. As one can learn from Fig. 10, at the critical value of the actuation amplitude w_c both equilibria coincide and are unstable with respect to any infinitesimal disturbances (marginally stable), so that the bubble grows with time and becomes unbounded for $t \to \infty$. For $w > w_c$ there are two equilibria points: one is unstable and the other is stable. The latter corresponds to the situation when the bubble is of finite size, and this state has a finite domain of attraction. Note that the potential energy shape, as in Fig. 9, is crucial in allowing the "dynamic" bifurcation: a V-shaped potential function apparently would not allow this type of bifurcation; in addition the domain of attraction would be modeled inconsistently with physics. A similar type of argument will be applied to the hysteresis phenomena in Section 4. In conclusion, having identified, based on physical arguments, that the potential should be of the shape as in Fig. 9 in order to allow a dynamic bifurcation, the problem reduces to determination of the coefficients in (4). This general procedure is the subject of the singularity theory [11].

3.4.4. The model and its interpretation

For simplicity, restricting ourselves to the case of thick airfoils when separation occurs at $\alpha_c = 0$ without actuation, with one of infinitely many admissible choices of b and c we get

$$\ddot{x} + \mu\dot{x} = -V_x(x; \alpha, w) = (x - \alpha)^2 + f(w)\, x. \tag{5}$$

Here $f(w) = a_1 w + a_2 w^2 + \cdots$ represents a *nonlinear response* of the separation region to actuator excitations w. The product $f(w)\, x$ implies that the effect of actuation depends upon the bubble size x. As required, $f(w_c) = 2\alpha^{1/2}$ and the bubble shrinks as $\sim f^{-1}$

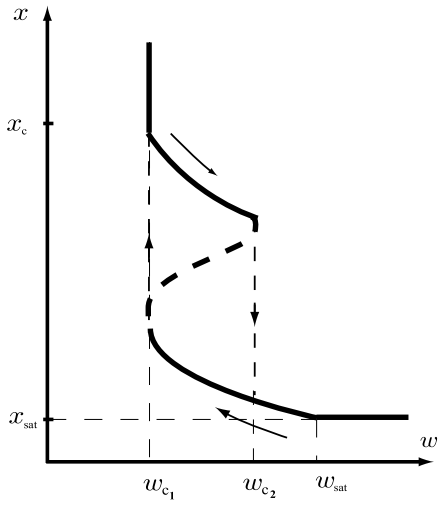

Fig. 11. Experimental effect of time-varying actuation: Hysteresis phenomenon as it depends on the amplitude w.

for $w \to \infty$. While this is the simplest possibility, from the above description it is clear that there is enough flexibility to calibrate the model through the fitting functions, $F(x, w, \alpha)$, and parameters, $(b, c, \ldots)$ within the bounds given above.

By construction, the model (5) reflects the basic generic dynamic behavior of separation bubbles. In the *conservative* time-invariant case the parametric space is just $(\alpha, f(w))$. When control is absent, $f(w) = 0$, the bubble is open, which corresponds to an unstable phase portrait in Fig. 8(a); that is, any initial conditions lead to an unbounded bubble size x. When sufficient control is applied (consider first α fixed), the bubble closes, which is reflected in the change of the phase portrait as shown in Fig. 8(b). In this case there are two equilibrium points: one is a saddle, which is unstable and thus not physically observable, and the other is a stable center. Therefore, there exists a non-zero basin of attraction which leads to a finite bubble size, $x < \infty$. Fig. 8(b) also suggests that the system is susceptible to a finite-amplitude instability for $w > w_c$, a fact which is conceivable but has never been studied in experiments systematically. Nevertheless, it is known empirically that the bubble opens if the actuation amplitude becomes large enough, as in Fig. 6; see also [22]. Also, the fact that the boundary layer is susceptible to finite-amplitude instabilities [23] suggests that the separation bubble formed out of it may also be finite-amplitude unstable. The inclusion of dissipation in the model (5) does not change the nature of the phase portrait; however, it does change the basin of attraction.

Finally, the inclusion of time-varying effects in the control, $w = w_0 \cos \omega t$ with $\omega \neq 0$, also demonstrates that the bubble transforms from an open to a closed state. Thus, as required, the model (5) captures the primary bifurcation and dynamic behavior of the separation bubble, except for the phenomenon of hysteresis. In the rest of this paper we will explain how the model (5) can be *enhanced* to account for the hysteresis shown in Fig. 11. While the model (5) is illustrated for a particular choice of coefficients in (3), there is obviously enough freedom to choose parameters, which is important in order to fit the model to a particular application via calibration.

It is notable that a model of a similar form was deduced in an ad hoc way for a real bubble deforming in a straining flow of Taylor's four-roll mill studied by Kang and Leal [10]. This system experiences a bifurcation from a deformed but closed state to an open tip-streaming state, when the original bubble forms pointed open ends that emit tiny bubbles.

4. Hysteresis in the dynamics of separation bubble

4.1. Experimental observations: The model objectives

The basic effects of time-varying control were discussed in Section 3.3 and reflected in Fig. 6. However, the effect of changing amplitude and frequency is not trivial in view of the presence of a hysteresis [24,25] in all variables (α, w, ω), as illustrated in Fig. 11 for the dependence of the bubble size on the actuation amplitude, $x(w)$. Experiments demonstrate that hysteresis is present no matter how slowly the actuation amplitude w is changed, which suggests that the model should depend only on the sign of the rate $\dot{w}$.

Therefore, the model should reflect the fact that there are two stable steady state solutions for the range of the control parameter $w_{c_1} < w < w_{c_2}$, as in Fig. 11, which is an experimental fact. Mathematically, this means that the selection between these two solutions is due to the placement of initial conditions in the corresponding domain of attraction. Also, for $w > w_{c_2}$, there should be only one stable solution, while for $w < w_{c_1}$ the bubble should "bifurcate" to infinity in a dynamical manner, as described in Section 3.4. The challenge of modeling the hysteresis, similar to that of bifurcation, comes from the fact that there are no analytical results on the behavior of the bubble. In particular, the domain of attraction of stable solutions is not well characterized from the existing empirical data.

Therefore, in order to model hysteresis, one first needs to understand its physical origin, which is addressed below, in Section 4.2, where we suggest the physical mechanisms of hysteresis. This together with the dynamical systems and singularity theory allow us to modify the model (5) to account for hysteresis, which is the subject of Section 4.3.

4.2. On the physics of hysteresis

Physically, separation bubbles are caused by a strong adverse pressure gradient, which makes the boundary layer separate from the curved airfoil surface. Actuation with $w > w_c$ effectively reduces the adverse pressure gradient[3] and makes the bubble closed, as in Fig. 4(b). This can be seen from Bernoulli's equation, since the velocity drop is related to the pressure rise, $p + \rho u^2/2 = p_0$, where p is a dynamic pressure, and p_0 is the fluid pressure at rest. From Bernoulli's equation and Fig. 4 we can conclude that the pressure rise $p_i' - p_i''$ and bubble length l correlate $p_1' - p_1'' < p_2' - p_2''$ and $l_1 < l_2$, respectively. For current purposes we neglect the second-order effects of vorticity and thus assume constant pressure inside the bubble, $p_1 = p_2 = \text{const}$, which is the standard assumption when modeling the separated flow about an airfoil by Kirchhoff's zone of constant pressure [26,2].

Given the fact that the separation bubble boundary possesses elastic properties, see Section 3.4.2, we can provide a simple mechanistic explanation of the origin of the hysteresis. For simplicity, consider the two-dimensional situation depicted in Fig. 12: a hemispherical bubble having variable size with the left end fixed and with its right end free to move, thus modeling a separation bubble with moving reattachment point. The bubble size changes depending upon the free-stream velocity $u_{\max}$, which is chosen to be the control parameter. When $u_{\max}$ increases and the right end of the bubble reaches the trailing edge at R_0 at critical u_{cr}^2, the pressure inside the bubble increases by a finite amount, $p_0 \to p_0 + \Delta p_0$, which is due to suction of a high pressure fluid

[3] Note that for some airfoils the same effect can be achieved by changing the angle of attack α, i.e., the larger the angle of attack α, the stronger the adverse pressure gradient: this "interchangeability" of the effects of the actuation amplitude and the angle of attack is well known [21], and is reflected in the dependence $w_c(\alpha)$.

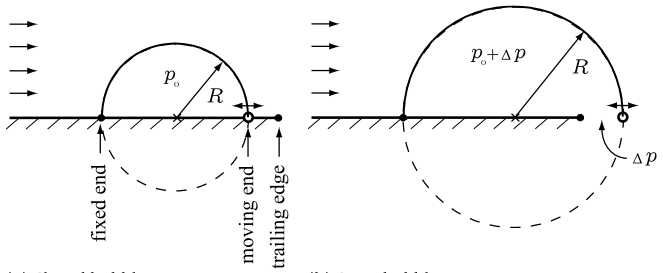

(a) Closed bubble. (b) Open bubble.

Fig. 12. Mechanical model of separation bubble hysteresis.

from the lower side of the airfoil. Hence the bubble size increases abruptly by some amount. Conversely, when $u_{\max}$ decreases and the bubble reaches the trailing edge at R_0 at a different critical $u^1_{\rm cr}$, the pressure inside the bubble relaxes to its original value, $p_0 \to p_0 - \Delta p_0$. The jump in pressure at the critical point – when reattachment is at the trailing edge – has the following physical explanation. It is known that the lift drops when the bubble opens, which effectively means that the pressure balance between the lower and upper surfaces of an airfoil has changed: some amount of pressure at the lower surface has leaked into the upper surface, namely into the bubble. The latter is allowed by unsteadiness of the process, i.e., the unsteady Kutta–Joukowsky condition.

Therefore, the mechanical analog of a separation bubble is $p = p_0 + \widetilde{\sigma}/R, p > p_0$, so that the bubble grows when the ambient pressure dictated by Bernoulli's equation, $p = p_\infty - \rho u^2_{\max}/2$, decreases:

$$u^2_{\rm cr}\ (\dot u_{\max} > 0) : R_0 = \frac{\widetilde{\sigma}}{p_\infty - p_0 - \frac{\rho (u^2_{\rm cr})^2}{2}}, \tag{6a}$$

$$u^1_{\rm cr}\ (\dot u_{\max} < 0) : R_0 = \frac{\widetilde{\sigma}}{p_\infty - p_0 - \Delta p_0 - \frac{\rho (u^1_{\rm cr})^2}{2}}, \tag{6b}$$

which produces a hysteretic behavior; see Fig. 13. Obviously, $u^1_{\rm cr} < u^2_{\rm cr}$ is consistent with physical observations.

In the light of the above, one can account for the hysteresis in Fig. 11 in model (5) as follows. When $\dot w < 0$ and w passes through w_c the transformation $w \to w - \Delta w$ with $\Delta w > 0$ is applied, since physically the effectiveness of control drops by Δw. When $\dot w > 0$ and $w = w'_c$ then $w \to w + \Delta w$, since a too conservative amount of control has been applied before reaching $w = w'_c$. These altogether lead to the desired hysteretic behavior. The same can be done to account for the hysteretic dependence on the angle of attack α.

The above mechanistic model of hysteresis captures the physics and proves that the separation bubble has a non-trivial potential function associated with it. It should be noted that such discontinuous modeling of hysteresis based on the rate sign $\dot w$ is still widely used in applications and known as *play* and *stop* (classical Prandtl model) models; see Visintin [27].

4.3. Accounting for hysteresis in model (5)

However, for the purpose of deriving a universal model which combines both the bifurcation and the hysteresis in a dynamic manner, i.e. suitable for control purposes, it makes sense to follow another way of modeling hysteresis phenomena, based on the construction of an appropriate potential function $V(x)$, similar to what was done in Section 3.4.

The grounding thesis is that the true curve of states in Fig. 11 is not the solid discontinuous one, but rather the "true" picture for separation bubbles corresponds to the smooth curve (including the dashed line portion) in Fig. 11, a fact which has not been realized

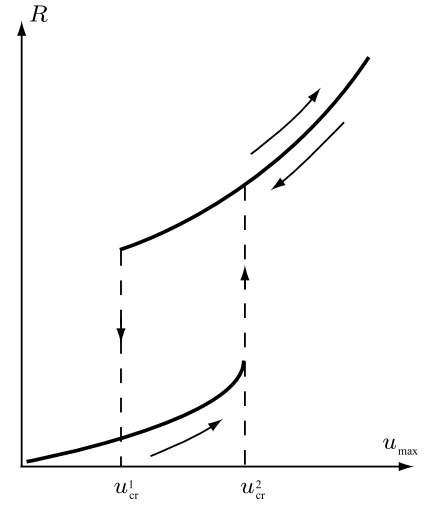

Fig. 13. Schematics of model (6) for hysteresis.

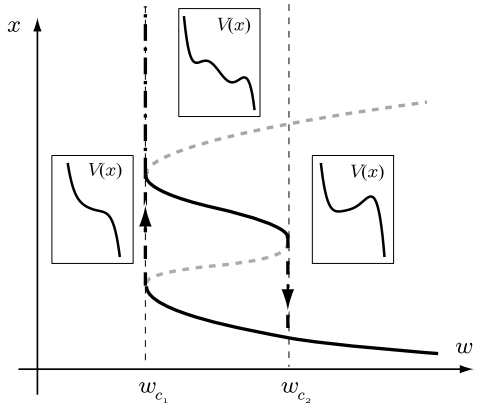

Fig. 14. Hysteresis curve in the (x, w)-plane and corresponding potential functions; solid black lines represent stable equilibria, while dashed lines are unstable equilibria; the dot–dash line represents a dynamic bifurcation (the bubble size grows with time unboundedly). The $V(x)$ plots in rectangles show the shape of the potential for $w < w_{c_1}$, $w \in [w_{c_1}, w_{c_2}]$, and $w > w_{c_2}$, respectively.

in the literature on separation bubbles before.[4] This smooth curve corresponds to the equilibria states of an appropriate potential function $V(x)$; the dashed curve is not physically observable in view of the instability of the corresponding equilibrium states. From Section 3.4 we know that the potential function should be of special shape, i.e. when $x \to \pm\infty$, then $V(x) \to \mp\infty$, that is the highest-order terms in α should be odd. Then, as a natural generalization of the picture in Fig. 10, we arrive at Fig. 14.

At the technical level, the lowest-order potential suitable for achieving the picture in Fig. 14 is of the fifth order, so model (5) becomes

$$\ddot x + \mu \dot x = -V_x(x; \alpha, w), \tag{7}$$

with V being the fifth-order polynomial of x. The existence of such a potential is apparent, and its coefficients in the polynomial representation can be found with the help of linear programming given a set of inequalities and equalities based on the calibration requirements. By design, model (7) accounts for the observed hysteretic behavior; see Section 4.2.

In conclusion, the fact that the hysteresis originates from the particularity of the potential function is well known from

[4] However, this fact is known in other physical situations: e.g. a ferromagnetic drop deforming in a magnetic field [28] and cavitating hydrofoils [29].

other physical systems, e.g. a ferromagnetic drop deforming in a magnetic field [28] and cavitating hydrofoils [29]. For example, the ferromagnetic drop shape is a simple balancing between magnetic and interfacial energy of the drop: the former tends to elongate the drop, while the latter tends to make the drop spherical, which leads to hysteretic behavior. In the case of a cavitation bubble on a hydrofoil, the hysteresis can be explained with the help of inviscid free-streamline theory [30,31] since the boundary of the bubble is well defined physically: the predictions of the free-streamline theory [32] agree well with experiments [33].

5. Conclusions

This work has focused on the fundamental aspects—the most important physical and dynamic behavior—of a generic separation bubble using thick airfoils as a paradigm. Given an incomplete experimental knowledge of the complex phenomena of separation bubble, we applied the deduction based on bifurcation and singularity theories and thus (i) filled in incomplete pieces in the dynamical picture of the phenomena, (ii) advocated that this dynamical picture is finite dimensional at the coarse level, (iii) developed a constructive way of building a model, and (iv) deduced a model.

The model can be further enhanced in particular by (a) incorporating a non-trivial state equation of a bubble, (b) accounting for separation at non-zero angle of attack $a_c \neq 0$, and (c) calibrating the model for a given airfoil according to the procedure outlined in Sections 3.4.2 and 4.3. The approach taken here allows one to generalize models (5) and (7) hierarchically: e.g. to account for the three-dimensionality of a separation bubble one would need to introduce a second bubble size variable and to come up with physical reasonings on its dynamics. These are the potential future directions of this study and will require considerable theoretical and experimental efforts. We also expect that this approach to low-dimensional modeling will be helpful in real-time flow control.

Acknowledgements

R.K. would like to thank Prof. Anatol Roshko for helpful and encouraging discussions. This work was supported in part by NSF-ITR Grant ACI-0204932.

References

[1] T. Kailath, Linear Systems, Prentice-Hall, 1980.
[2] M.G. Goman, A. Khrabrov, State-space representation of aerodynamic characteristics of an aircraft at high angles of attack, J. Aircraft 31 (1994) 1109–1115.
[3] M.G. Goman, A.V. Khramtsovsky, Application of continuation and bifurcation methods to the design of control, Philos. Trans. R. Soc. Lond. A 356 (1998) 2277–2295.
[4] V. Klein, K.D. Noderer, Modeling of aircraft unsteady aerodynamic characteristics, Technical Report NASA Tech. Mem. 109120, 1994.
[5] J. Magill, M. Bachmann, G. Rixon, K. McManus, Dynamic stall control using a model-based observer, J. Aircraft 40 (2003) 355–362.
[6] D. Petot, Differential equation modeling of dynamic stall, Rech. Aerosp. 5 (1989) 59–72.
[7] M. Tobak, G. T. Chapman, L. B. Schiff, Mathematical modelling of the aerodynamic characteristics in flight dynamics, Technical Report 85880, NASA TM, 1984.
[8] J. Guckenheimer, P. Holmes, Nonlinear Oscillations, Dynamical Systems, and Bifurcations of Vector Fields, Springer, 1983.
[9] R.S. Shaw, The Dripping Faucet as a Model Chaotic System, Arial, Santa Cruz, 1984.
[10] I.S. Kang, L.G. Leal, Bubble dynamics in time-periodic straining flows, J. Fluid Mech. 218 (1990) 41–69.
[11] V.I. Arnold, Bifurcation Theory and Catastrophe Theory, Springer-Verlag, New York, 1999.
[12] H. Schlichting, K. Gersten, Boundary Layer Theory, Springer-Verlag, 2000.
[13] B.M. Jones, Stalling, J. Roy. Aero. Soc. 38 (1934) 753–770.
[14] L.L. Pauley, P. Moin, W.C. Reynolds, The structure of two-dimensional separation, J. Fluid Mech. 220 (1990) 397–411.
[15] I. Tani, Low-speed flows involving bubble separations, Prog. Aero. Sci. 5 (1964) 70–103.
[16] M. Ghil, J.-G. Liu, C. Wang, S. Wang, Boundary-layer separation and adverse pressure gradient for 2d viscous incompressible flow, Physica D 197 (2004) 149–173.
[17] G.L. Brown, A. Roshko, On density effects and large structure in turbulent mixing layers, J. Fluid Mech. 64 (1974) 775–816.
[18] D. Oster, I. Wygnanski, The forced mixing layer between parallel streams, J. Fluid Mech. 123 (1982) 91–130.
[19] A. Seifert, L.G. Pack, Active flow separation control on wall-mounted hump at high Reynolds numbers, AIAA J. 40 (2002) 1363–1372.
[20] P. Mereau, R. Hirsh, G. Coulon, A. Rault, Identification of unsteady effects in lift build up, Technical Report AGARD-CP-235, 1978.
[21] M. Amitay, A. Glezer, Role of actuation frequency in controlled flow. Reattachment over a stalled airfoil, AIAA J. 40 (2002) 209–216.
[22] R. Krechetnikov, I.I. Lipatov, Time-periodic boundary layer under conditions of the large amplitude external disturbances, Trans. Central Aero-Hydrodynamics Inst. 31 (2000) 27–40.
[23] A.H. Nayfeh, Nonlinear stability of boundary layers, in: Aerospace Sciences Meeting, 25th, Reno, NV, Jan 12–15, 1987, pp. 1–54.
[24] B. Nishri, I. Wygnanski, Effects of periodic excitation on turbulent flow. separation from a flap, AIAA J. 36 (1998) 547–556.
[25] D. Greenblatt, B. Nishri, A. Darabi, I. Wygnanski, Dynamic stall control by periodic excitation. Part 2: Mechanisms, J. Aircraft 38 (2001) 439–447.
[26] M.I. Gurevich, Theory of Ideal Fluids Jets, Nauka, Moscow, 1979.
[27] A. Visintin, Differential Models of Hysteresis, Springer, 1994.
[28] J.-C. Bacri, D. Salin, Instability of ferrofluid magnetic drops under magnetic field, J. Phys. Lett. 43 (1982) 649–654.
[29] V.V. Sychev, High Reynolds number flow past a plate mounted at a small angle of attack, Fluid Dynam. 36 (2001) 244–261.
[30] A.J. Acosta, A note on partial cavitation of flat plate, Technical Report E-19.9, Hydrodynamic Laboratory, California Institute of Technology, 1955.
[31] M.P. Tulin, Steady two-dimensional cavity flows about slender bodies, Technical Report 834, David Taylor Model Basin, 1953.
[32] J.A. Geurst, Linearized theory for partially cavitated hydrofoils, Int. Shipbuilding Progr. 6 (1959) 369–384.
[33] M.C. Meijer, Some experiments on partly cavitating hydrofoils, Int. Shipbuilding Progr. 6 (1959) 361–368.